JOURNAL OF BACTERIOLOGY, Dec. 2007, p. 8741–8745 Vol. 187, No. 23
0021-9193/07/$08.00+0 doi:10.1128/JB.01130-07

H_2O_2 Is Required for Optimal Establishment of the *Medicago sativa*/*Sinorhizobium meliloti* Symbiosis▽

Alexandre Jamet,† Karine Mandon, Alain Puppo, and Didier Hérouart*

Interactions Plantes-Microorganismes et Santé Végétale, UMR IPMSV INRA 1064 – CNRS 6192, Université de Nice—Sophia Antipolis, Centre Sophia Agrobiotech, 400 route des chappes, BP 167, F-06903 Sophia Antipolis, France

Received 18 July 2007/Accepted 20 September 2007

The symbiotic interaction between *Medicago sativa* and *Sinorhizobium meliloti* Rm*katB*$^{++}$ overexpressing the housekeeping catalase *katB* is delayed, and this delay is combined with an enlargement of infection threads. This result provides evidence that H_2O_2 is required for optimal progression of infection threads through the root hairs and plant cell layers.

Leguminous plants can engage in a symbiotic interaction with *Rhizobia* and form new root organs, the nodules. The nodulation process is initiated by a complex signal exchange between both partners (5). Rhizobial invasion in the symbiotic model *Medicago sativa*/*Sinorhizobium meliloti* occurs via root hairs. The perception of bacterial nodulation factors by the host plant leads to cell division in the root pericycle and in the root cortex, where the nodule primordium forms. Simultaneously, root hairs deform and curl. The bacteria are entrapped in this curl, local cell wall is hydrolyzed, and a plasma membrane invagination occurs, leading to the formation of an infection thread (IT) (3). This plant-derived tubule filled with dividing and growing bacteria first progresses through the infected root hair and then traverses several cell layers toward the nodule primordium. Bacterial cells at the tip of the IT are released and enclosed in peribacteroid membranes in the host cell cytoplasm (10). Once inside the plant cells, the bacteria differentiate into nondividing nitrogen-fixing endosymbionts called bacteroids, which are able to fix atmospheric dinitrogen (22).

Important progress has recently been made in analyzing the mechanisms that initiate the establishment of the symbiosis and especially the mechanism of the perception of bacterial nodulation factors by the host plants (12, 18). The development of an IT inside root hair and the architecture of IT networks in nodules have been recently studied (9, 21). In fact, ITs can be considered as tubular ingrowths of the plant cell wall. In pea/*Rhizobium leguminosarum* symbiosis, a family of extensin-like glycoproteins associated with the lumen of these ITs has been identified (25). However, more data are necessary to clearly identify the biochemical mechanisms by which ITs grow. Reactive oxygen species like O_2^- and H_2O_2 could be implicated, since they have been implicated during the infection process and especially in the ITs (28). The observed distribution of H_2O_2 in ITs and the plant cell wall strongly suggests that H_2O_2 is of plant origin (30). To overcome this reactive oxygen species production, *S. meliloti* possesses at least two superoxide dismutases (SodA and SodC) and three catalases (KatA, KatB, and KatC). It has been shown that the corresponding genes are differentially expressed not only during free-living growth but also during nodule establishment. Indeed, both *sod* genes are expressed in ITs (27; D. Touati, personal communication). In contrast, only *katB* and *katC* genes, and not the uniquely H_2O_2-inducible *katA* gene (15), are strongly expressed in the ITs despite the detection of H_2O_2 all around the bacteria (16). Moreover, a nonefficient release into plant cells and a perturbed differentiation of bacteria into bacteroids have been observed for a *katB katC* double mutant (16). In free-living conditions, the coexpression of *katB* and *katC* has been observed only during the stationary phase, suggesting that most of bacteria within the ITs are potentially in a nonexponential growth phase. This has recently been corroborated by experiments showing that bacterial growth occurs only in a very small region on the tip of ITs (9). Moreover, on the basis of observations of root tips, the potential implication of H_2O_2 in an insolubilization of the glycoprotein matrix within IT lumen has been suggested (30).

To further comprehend the mechanisms of IT growth, we tried to modify the H_2O_2 content within IT by using an *S. meliloti* strain overexpressing one catalase. Among the three catalases, KatB was selected because it plays a housekeeping role, as it is expressed throughout all the growth phases of the free-living bacterium and also during symbiosis. Moreover, KatB shows a higher affinity for H_2O_2 than the two other catalases of *S. meliloti* (1). In order to overexpress KatB, the *Salmonella enterica* serovar Typhimurium *trp* promoter was fused upstream of the complete coding region of *katB* by four cloning steps. The first of these consisted of amplification of the *katB* open reading frame by PCR using the following primers: AJKATB1 (5′-CC**ATCGAT**CGCCCAATCGAGGAAGAGG-3′), creating a new ClaI restriction site, and AJKATB2 (5′-ACATGGG**CTCGAG**CCACGT-3′), creating a new XhoI restriction site (boldface in sequences indicates restriction sites). Subsequent steps included subcloning in pGEM-T (Promega corporation), double digestion ClaI and XhoI, and in-

* Corresponding author. Mailing address: Interactions Plantes-Microorganismes et Santé Végétale, UMR IPMSV INRA 1064 – CNRS 6192, Université de Nice—Sophia Antipolis, Centre Sophia Agrobiotech, 400 route des chappes, BP 167, F-06903 Sophia Antipolis, France. Phone: (33) 492 38 66 36. Fax: (33) 492 38 66 40. E-mail: herouart@unice.fr.

† Present address: Unité de Recherche en Biologie Moléculaire (URBM), Facultés Universitaires Notre-Dame de la Paix, rue de Bruxelles 61, B-5000 Namur, Belgium.

▽ Published ahead of print on 5 October 2007.

TABLE 1. Catalase activity and symbiotic performance of Rm1021 and Rm*katB*$^{++}$ strains

S. meliloti strain	Catalase activity[a]		No. of nodules per 72 plants at[b]:	
	Exponential phase	Stationary phase	7 dpi	14 dpi
Rm1021	32 ± 7.1	21 ± 3.5	24.5 ± 3.7	80.6 ± 7.5
Rm*katB*$^{++}$	90.1 ± 14	203 ± 43	8.3 ± 4.3	55.2 ± 12.4

[a] Values are means ± standard errors obtained from triplicate samples of two independent experiments and are given in units per milligram of protein.

[b] Values are means ± standard errors and were obtained from three independent experiments. The nodules were counted at 7 and 14 days postinoculation (dpi).

sertion into pTB93F (11) to create the pTB*katB*$^{++}$ plasmid. The efficiency of the *trp* promoter to overproduce KatB has been tested by transferring this recombinant plasmid into the recipient *katB*-null mutant GKBZ01 expressing a p*katB-lacZ* fusion by triparental mating. Total catalase activities were 36 ± 6.7, 17 ± 7.2, and 380 ± 102 U/μg of protein in crude extracts of GMI211, GKBZ01, and GKBZ01/pTB*katB*$^{++}$, respectively, indicating that the *trp* promoter allows a 10-fold increase in the catalase activity in *S. meliloti*. However, the recombinant plasmid was unstable in *S. meliloti* during the plant infection process without antibiotic pressure (data not shown).

To avoid this problem, the chimeric construction allowing the overexpression of *katB* was integrated into the pSymA megaplasmid by recombination. Four more cloning steps were necessary before the transfer by triparental mating. The BamHI/BglII fragment of the pTB*katB*$^{++}$ plasmid, containing the p*trp* promoter and 80% of the KatB open reading frame, was subcloned into the BamHI site of the pSUP202 plasmid, resulting in the pSUP*katB*$^{++}$ plasmid. A *lacZ*/Nm^{r} cassette extracted from the pKOK5 plasmid was inserted into the SalI restriction site of pSUP*katB*$^{++}$, resulting in the pSUP*katB*$^{++}$*lacZ* plasmid. The recombinant Rm*katB*$^{++}$ strain expressing both p*katB-lacZ* and p*Trp-katB* fusions was obtained by triparental mating using the Rm1021 wild-type strain as that recipient strain. Expression levels of *trp* and *katB* promoters in the ITs are not known, and it was impossible to accurately measure the catalase activity from IT bacteria. However, the catalase capacities of free-living Rm*katB*$^{++}$ were determined during growth in Luria-Bertani medium containing 2.5 mM $MgSO_4$ and 2.5 mM $CaCl_2$ (LB-MC). During the exponential phase, the total catalase activity in Rm*katB*$^{++}$ was three times higher than that in Rm1021, whereas a 10-fold increase was observed during the stationary phase (Table 1). Analysis of the catalase activity pattern on native polyacrylamide gel by use of inhibition of diaminobenzidine oxidation by H_2O_2 (14) showed that the increase of total catalase activity in the stationary phase was largely due to an increase of KatB (Fig. 1A and B). To evaluate the resistance of Rm*katB*$^{++}$ to exogenous H_2O_2, the survival of bacteria was checked by incubating for 30 min in LB-MC containing an increasing concentration of H_2O_2. The treatment was stopped by adding exogenous catalase, and bacteria were counted on the LB-MC plate. In the presence of 10 mM H_2O_2, wild-type Rm1021 bacteria were rapidly killed, whereas the survival of recombinant Rm*katB*$^{++}$ cells was only slightly reduced (data not shown). The intracellular concentration of H_2O_2 was evaluated in both strains by use of an Amplex Red kit (Molecular Probes, Montluçon, France) as described previously for *Agrobacterium tumefaciens* (31). H_2O_2 concentrations of 124 nM and 52 nM in Rm1021 and Rm*katB*$^{++}$, respectively, were estimated, indicating that the mutant strain has a lower internal H_2O_2 level.

To test the effect of *katB* overexpression on the symbiotic process, the symbiotic performance of recombinant Rm*katB*$^{++}$ strain to its parental wild type was assessed by three independent experiments. The number of nodules per 72 plants was determined 7, 14, and 21 days after inoculation with the mutant Rm*katB*$^{++}$ strain and with Rm1021 as the control. The values obtained for 7 and 14 days postinoculation indicate that the Rm*katB*$^{++}$ strain presents a delayed nodulation phenotype following the infection (Table 1). Moreover, this delay does not appear to be due to a modification of the early steps of the infection process, since the expression levels of early plant nodulin genes *ENOD12* (24) and *MtN6* (20), determined by reverse transcription-PCR using total RNA from *M. truncatula* root tips, were found to be similar for infection with Rm1021 and Rm*katB*$^{++}$ (data not shown). However, 3 weeks after infection, no significant difference between plants inoculated with Rm1021 or Rm*katB*$^{++}$ was observed in terms of the number of nodules and the capacity of bacteroids to reduce the dinitrogen within nodules (data not shown). To determine more precisely the point at which the Rm*katB*$^{++}$ strain is affected during the infection process, the plasmid pXLGD4 (17), which contains a *hemA-lacZ* fusion allowing a constitutive expression of *lacZ*, was transfected into the Rm1021 and Rm*katB*$^{++}$ strains. A set of 40 plants were infected for each strain, and the efficiency of infection was estimated 5 days after infection using the following criteria: colonized curled root hairs, initiated ITs, extended ITs, and infected young nodules (Fig. 2). The global numbers of infection events were similar for both strains. In contrast, the number of extended ITs and the ratio of initiated ITs to colonized curled root hairs were significantly higher for Rm1021/pXLGD4 than for Rm*katB*$^{++}$/pXLGD4. Moreover, the ITs showed an irregular aspect and a larger average diameter for Rm*katB*$^{++}$ (7.34 ± 2.25 μm) than for Rm1021 (3 ± 1.07 μm). The diameters of 40 ITs from each strain were measured using images from bright-field microscopy (Fig. 3). H_2O_2 accumulation was analyzed in ultrathin sections of ITs of very young nodules as an electron-dense deposit stained with cerium chloride as describe previously (2, 28). When plants were infected with Rm1021, H_2O_2 was detected in most of the ITs, principally between the cell wall and the matrix (Fig. 4A and B).

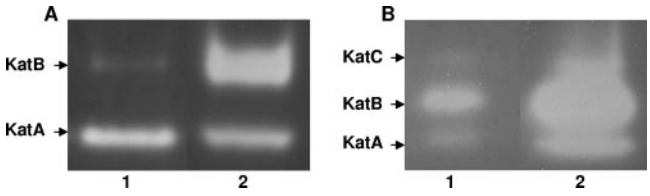

FIG. 1. Catalase activity of *Sinorhizobium meliloti* strains: Rm1021 (lane 1) and Rm*katB*$^{++}$ (lane 2) in exponential (A) and stationary (B) phases. The locations of KatA, KatB, and KatC are indicated according to the work of Sigaud et al. (29). Twenty-five micrograms of total protein was loaded on each lane.

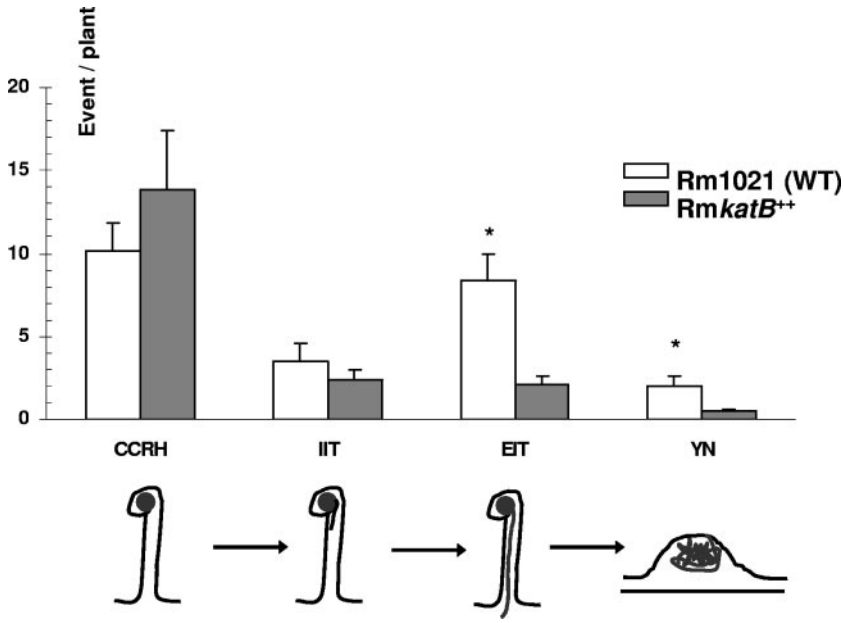

FIG. 2. Number of infection events 5 days after infection with Rm1021 and Rm*katB*$^{++}$ strains. Experimental data were assessed for statistical significance by means of the Student *t* test; ∗ indicates significant difference ($P < 0.05$). Abbreviations: CCRH, colonized curled root hair; IIT, initiated IT; EIT, extended ITs; YN, young nodule; WT, wild type.

In contrast, no H_2O_2 could be observed in enlarged ITs obtained with Rm*katB*$^{++}$, whereas the peroxide is still detectable in the cell wall (Fig. 4C and D). This indicates that the mutant has an enhanced ability to inactivate H_2O_2 associated with IT walls. As a control, the detection of H_2O_2 in ITs was completely abolished by treating the sample with 25 μg ml^{-1} of catalase before adding cerium chloride, indicating that it reflects H_2O_2 accumulation (data not shown).

Other bacterial mutant strains have been shown also to exhibit a nodulation-delayed phenotype similar to that of Rm*katB*$^{++}$, particularly those affected in their production of exopolysaccharides (4, 6, 8, 23). To determine if the exopo-

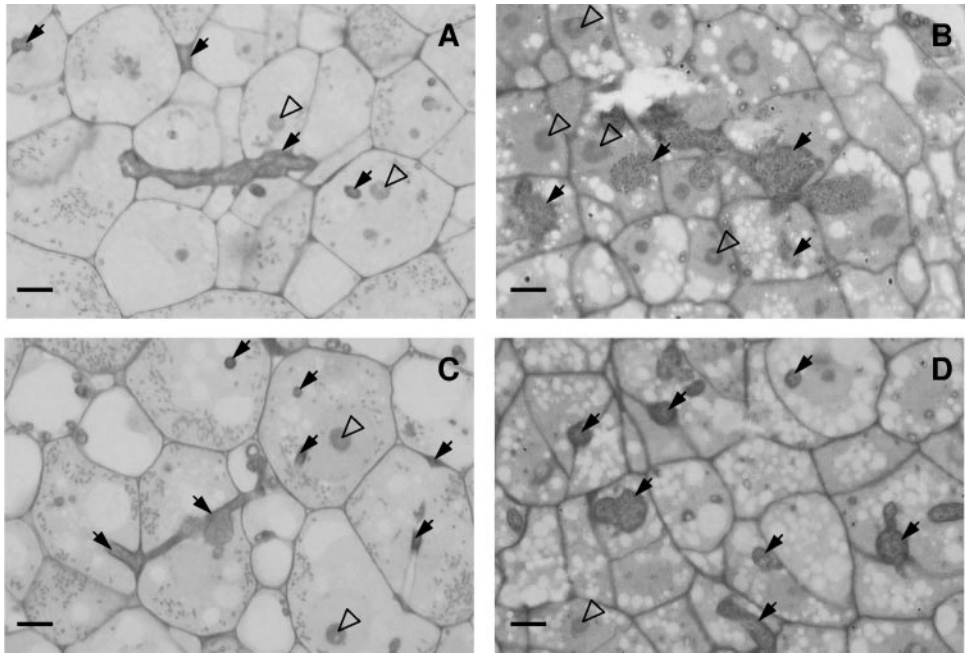

FIG. 3. Structure of ITs in 5-day-old nodules. Nodules were induced by the Rm1021 (A and C) and Rm*katB*$^{++}$ (B and D) strains. Black arrows show ITs, and open arrowheads show nuclei. Scale bars = 10 μm.

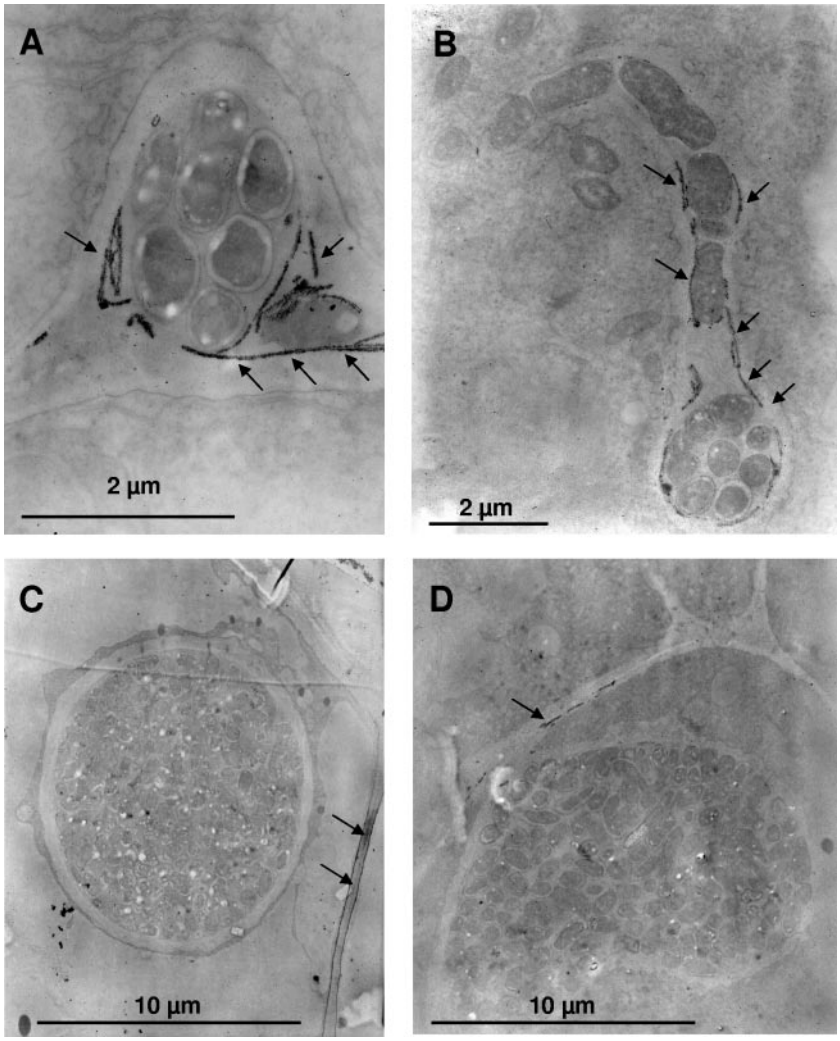

FIG. 4. Detection of H_2O_2 accumulation as electron-dense precipitate formed in the presence of cerium chloride (arrows) in ITs 5 days after infection with Rm1021 (A and B) and Rm*katB*$^{++}$ (C and D). (A, C, and D) Transversal cross section of ITs. (B) Longitudinal cross-section showing the release of bacteria inside the plant cell. Magnitudes of pictures are indicated with scale bars.

lysaccharide content was affected in Rm*katB*$^{++}$, two distinct tests were performed: one with the UV-fluorescent calcofluor, which binds a portion of succinoglycan (7), and the other with Sudan black B, which detects the galactoglucan and some succinoglycan, which are not involved in calcofluor fluorescence (19). No difference between Rm1021 and Rm*katB*$^{++}$ was observed, indicating that the phenotype observed for Rm*katB*$^{++}$ could not be explained simply by a modification of exopolysaccharide production (data not shown).

In conclusion, our results indicate that the H_2O_2 production observed within some ITs (28), which did not appear to induce an oxidative stress for bacteria (16), has a crucial role in optimizing IT development. This is in line with the hypothesis of an important H_2O_2 involvement in the biomechanics of IT growth via the cross-linking of glycosylated plant glycoproteins, namely, the root nodule extensins, which are localized in the extracellular matrix of legume tissues and in the lumen of ITs (13, 30). The reduced levels of H_2O_2 in the ITs obtained with Rm*katB*$^{++}$ could influence the rate of cross-linking of these extensins, compromising a polarized growth of ITs and leading to their enlargement. The results presented here are in agreement with an early report by Salzwedel and Dazzo (26), where peroxidase activities were localized during root hair infection and were supposed to contribute to the infection process.

We gratefully acknowledge G. Van de Sype for technical help on ultramicroscopic analyses and Julie Hopkins for help with proofreading.

A. Jamet's work was supported by a grant from the Ministère de l'Education National, de l'Enseignement supérieur et de la Recherche.

REFERENCES

1. **Ardissone, S., P. Frendo, E. Laurenti, W. Jantschko, C. Obinger, A. Puppo, and R. P. Ferrari.** 2004. Purification and physical-chemical characterization of the three hydroperoxidases from the symbiotic bacterium Sinorhizobium meliloti. Biochemistry **43:**12692–12699.
2. **Bestwick, C. S., I. R. Brown, M. H. Bennett, and J. W. Mansfield.** 1997. Localisation of hydrogen peroxide accumulation during the hypersensitive reaction of lettuce cells to *Pseudomonas syringae* pv *phaseolicola*. Plant Cell **9:**209–221.
3. **Brewin, N. J.** 2004. Plant cell wall remodelling in the *Rhizobium*-legume symbiosis. Crit. Rev. Plant Sci. **25:**1–24.

4. **Cheng, H.-P., and G. C. Walker.** 1998. Succinoglycan is required for initiation and elongation of infection threads during nodulation of alfalfa by *Rhizobium meliloti*. J. Bacteriol. **180:**5183–5191.
5. **Denarie, J., F. Debelle, and J. C. Prome.** 1996. Rhizobium lipo-chitooligosaccharide nodulation factors: signaling molecules mediating recognition and morphogenesis. Annu. Rev. Biochem. **65:**503–535.
6. **D'Haeze, W., J. Glushka, R. De Rycke, M. Holsters, and R. W. Carlson.** 2004. Structural characterization of extracellular polysaccharides of *Azorhizobium caulinodans* and importance for nodule initiation on *Sesbania rostrata*. Mol. Microbiol. **52:**485–500.
7. **Doherty, D., J. A. Leigh, J. Glazebrook, and G. C. Walker.** 1988. *Rhizobium meliloti* mutants that overproduce the *R. meliloti* acidic calcofluor-binding exopolysaccharide. J. Bacteriol. **170:**4249–4256.
8. **Fraysse, N., F. Couderc, and V. Poinsot.** 2003. Surface polysaccharide involvement in establishing the rhizobium-legume symbiosis. Eur. J. Biochem. **270:**1365–1380.
9. **Gage, D. J.** 2002. Analysis of infection thread development using Gfp- and DsRed-expressing *Sinorhizobium meliloti*. J. Bacteriol. **184:**7042–7046.
10. **Gage, D. J.** 2004. Infection and invasion of roots by symbiotic, nitrogen-fixing rhizobia during nodulation of temperate legumes. Microbiol. Mol. Biol. Rev. **68:**280–300.
11. **Gage, D. J., T. Bobo, and S. R. Long.** 1996. Use of green fluorescent protein to visualize the early events of symbiosis between *Rhizobium meliloti* and alfalfa (*Medicago sativa*). J. Bacteriol. **178:**7159–7166.
12. **Geurts, R., E. Fedorova, and T. Bisseling.** 2005. Nod factor signaling genes and their function in the early stages of Rhizobium infection. Curr. Opin. Plant Biol. **8:**346–352.
13. **Gucciardo, S., E. A. Rathbun, M. Shanks, S. Jenkyns, L. Mak, M. C. Durrant, and N. J. Brewin.** 2005. Epitope tagging of legume root nodule extensin modifies protein structure and crosslinking in cell walls of transformed tobacco leaves. Mol. Plant-Microbe Interact. **18:**24–32.
14. **Hérouart, D., S. Sigaud, S. Moreau, P. Frendo, D. Touati, and A. Puppo.** 1996. Cloning and characterization of the *katA* gene of *Rhizobium meliloti* encoding a hydrogen peroxide-inducible catalase. J. Bacteriol. **178:**6802–6809.
15. **Jamet, A., E. Kiss, J. Batut, A. Puppo, and D. Herouart.** 2005. The *katA* catalase gene is regulated by OxyR in both free-living and symbiotic *Sinorhizobium meliloti*. J. Bacteriol. **187:**376–381.
16. **Jamet, A., S. Sigaud, G. Van de Sype, A. Puppo, and D. Hérouart.** 2003. Expression of the bacterial catalase genes during *Sinorhizobium meliloti-Medicago sativa* symbiosis and their crucial role during infection process. Mol. Plant-Microbe Interact. **16:**217–225.
17. **Leong, S. A., P. H. Williams, and G. S. Ditta.** 1985. Analysis of the 5′ regulatory region of the gene for δ-aminolevulinic acid synthetase of *Rhizobium meliloti*. Nucleic Acids Res. **13:**5965–5976.
18. **Limpens, E., C. Franken, P. Smit, J. Willemse, T. Bisseling, and R. Geurts.** 2003. LysM domain receptor kinases regulating rhizobial Nod factor-induced infection. Science **302:**630–633.
19. **Liu, M., J. E. Gonzalez, L. B. Willis, and G. C. Walker.** 1998. A novel screening method for isolating exopolysaccharide-deficient mutants. Appl. Environ. Microbiol. **64:**4600–4602.
20. **Mathis, R., C. Grosjean, F. de Billy, T. Huguet, and P. Gamas.** 1999. The early nodulin gene MtN6 is a novel marker for events preceding infection of Medicago truncatula roots by Sinorhizobium meliloti. Mol. Plant-Microbe Interact. **12:**544–555.
21. **Monahan-Giovanelli, H., C. A. Pinedo, and D. J. Gage.** 2006. Architecture of infection thread networks in developing root nodules induced by the symbiotic bacterium Sinorhizobium meliloti on Medicago truncatula. Plant Physiol. **140:**661–670.
22. **Oke, V., and S. R. Long.** 1999. Bacterial genes induced within the nodule during the *Rhizobium*-legume symbiosis. Mol. Microbiol. **32:**837–849.
23. **Pellock, B. J., H.-P. Cheng, and G. C. Walker.** 2000. Alfalfa root nodule invasion efficiency is dependent on *Sinorhizobium meliloti* polysaccharides. J. Bacteriol. **182:**4310–4318.
24. **Pichon, M., E. P. Journet, A. Dedieu, F. de Billy, G. Truchet, and D. G. Barker.** 1992. Rhizobium meliloti elicits transient expression of the early nodulin gene ENOD12 in the differentiating root epidermis of transgenic alfalfa. Plant Cell **4:**1199–1211.
25. **Rathbun, E. A., M. J. Naldrett, and N. J. Brewin.** 2002. Identification of a family of extensin-like glycoproteins in the lumen of *Rhizobium*-induced infection threads in pea root nodules. Mol. Plant-Microbe Interact. **15:**350–359.
26. **Salzwedel, J. L., and F. B. Dazzo.** 1993. pSym *nod* gene influence on elicitation of peroxidase activity from white clover and pea roots by rhizobia and their cell-free supernatants. Mol. Plant-Microbe Interact. **6:**127–134.
27. **Santos, R., D. Hérouart, A. Puppo, and D. Touati.** 2000. Critical protective role of bacterial superoxide dismutase in *Rhizobium*-legume symbiosis. Mol. Microbiol. **38:**750–759.
28. **Santos, R., D. Hérouart, S. Sigaud, D. Touati, and A. Puppo.** 2001. Oxidative burst in alfalfa-*Sinorhizobium meliloti* symbiotic interaction. Mol. Plant-Microbe Interact. **14:**86–89.
29. **Sigaud, S., V. Becquet, P. Frendo, A. Puppo, and D. Hérouart.** 1999. Differential regulation of two divergent *Sinorhizobium meliloti* genes for HPII-like catalases during free-living growth and protective role of both catalases during symbiosis. J. Bacteriol. **181:**2634–2639.
30. **Wisniewski, J.-P., E. A. Rathbun, J. P. Knox, and N. J. Brewin.** 2000. Involvement of diamine oxidase and peroxidase in insolubilization of the extracellular matrix: implications for pea nodule initiation by *Rhizobium leguminosarum*. Mol. Plant-Microbe Interact. **13:**413–420.
31. **Xu, X. Q., L. P. Li, and S. Q. Pan.** 2001. Feedback regulation of an *Agrobacterium* catalase gene *katA* involved in *Agrobacterium*-plant interaction. Mol. Microbiol. **42:**645–657.